Journal of Breath Research

Online monitoring of carbon dioxide and oxygen in exhaled mouse breath via substrate-integrated hollow waveguide - Fourier transform infrared - luminescence spectroscopy

To cite this article before publication: Felicia Seichter *et al* 2018 *J. Breath Res.* in press https://doi.org/10.1088/1752-7163/aabf98

Online Monitoring of Carbon Dioxide and Oxygen in Exhaled Mouse Breath via Substrate-Integrated Hollow Waveguide - Fourier Transform Infrared - Luminescence Spectroscopy

Felicia Seichter[2], Erhan Tütüncü[2], Leila Tamina Hagemann[2], Josef Vogt[1], Ulrich Wachter[1], Michael Gröger[1], Sandra Kress[1], Peter Radermacher[1], Boris Mizaikoff[2*]

[1] Institute of Anesthesiologic Pathophysiology and Method Development, Ulm University Medical Center, Helmholtzstrasse 8/1, 89081 Ulm, Germany

[2] Institute of Analytical and Bioanalytical Chemistry, Ulm University, 89081 Ulm, Germany

E-mail: boris.mizaikoff@uni-ulm.de

Abstract. Exhaled breath offers monitoring bio markers, as well as diagnosing diseases and therapeutic interventions. In addition, vital functions may be non-invasively monitored on-line. Animal models are frequently used in research for determining novel therapeutic approaches and/or for investigating biological pathways. The exhaled carbon dioxide concentration, exhaled and inhaled oxygen concentration, and the subsequent respiratory quotient (RQ) offer insight into metabolic activity. One may adapt breath sampling systems and equipment designed for human applications to large animal studies, however, such adaptations are usually impossible for small animals due to their minuscule breath volume.

Here, we present a system for on-line monitoring of exhaled breath in a "mouse intensive care unit" (MICU) based on a modified Fourier-Transform infrared (FTIR) spectrometer equipped with a substrate integrated hollow waveguide (iHWG) gas cell, and a luminescence-based oxygen flow-through sensor integrated into the respiratory equipment of the MICU. Thereby, per-minute resolution of O_2 consumption and CO_2 production was obtained, and the 95% confidence range of the determined respiratory quotient was ±0.04 or approximately ±5% of the nominal value. Changes in the RQ value caused by intervention in either the metabolic or the respiratory system may therefore reliably be detected.

Keywords:

exhaled breath analysis, mouse, oxygen, carbon dioxide, FTIR, on-line monitoring, substrate-integrated hollow waveguide, iHWG, mid-infrared, luminescence sensing

1. Introduction

Apart from the determination of biomarker patterns serving as indication for certain conditions and diseases, the development of on-line analytical systems capable of quantifying or at least monitoring analytes in exhaled breath and relevant constituents in real time is among the major aims of breath analysis. On-line analysis promises to simplify sample collection as well as to avoid compromising samples [1]. As a non-invasive method and for on-line measurements, breath analysis is among the favored strategies vs, e.g., invasive blood sampling, which only provides a snapshot of the patient's condition. Carbon dioxide and oxygen are not only among the most abundant components in breath, but their concentration in exhaled breath also offers an important diagnostic into the metabolic status of a patient. Carbon dioxide is produced and released by the oxidation of carbohydrates, fats, and proteins. These oxidative processes also consume oxygen. Each of these processes consumes a specific amount of oxygen, and produces a specific amount of CO_2, which also generates a specific amount of heat. These contributions can be derived from literature, which are either based on stoichiometry or directly measured such as heat production after combustion. From these established physical principles, linear additive relations of oxygen consumption (VO_2 in mg/min) and CO_2 release (VCO_2 in mg/min), and associated oxidative loss of carbohydrates, loss of fat, and loss of protein (all losses in mg/min) as independent variables can be established. These equations can be rearranged to provide the so-called 'respiratory quotient' (RQ), i.e., the ratio of VCO_2 over VO_2 as a function of substrate utilization:

$$\mathrm{RQ} = \frac{\mathrm{VCO_2}}{\mathrm{VO_2}} = \frac{a_2}{a_3}\mathrm{f_{carb}} + \frac{b_2}{b_3}\mathrm{f_{fat}} + \frac{c_2}{c_3}\mathrm{f_{prot}} = \mathrm{f_{carb}} + 0.7\mathrm{f_{fat}} + 0.81\mathrm{f_{prot}} \quad (1)$$

where $\mathrm{f_{carb}}$ gives the relative contribution of the carbohydrate oxidation to VO_2. Other terms such as $\mathrm{f_{fat}}$ and $\mathrm{f_{prot}}$ are defined accordingly. Observed values for the RQ are rather insensitive to changes in the protein oxidation. Hence, if protein oxidation is replaced by a feasible mean constant value, the resulting error may be neglected [2]. Thus, feasible estimates for carbohydrate and fat oxidation may be obtained from RQ values alone. These metabolic parameters may then be used to exemplarily assess a shift from glucose oxidation

to fat oxidation, which provides a first and important information about the overall metabolic conditions [3,4].

There is a growing demand for breath diagnostics in animals either for veterinary diagnostics[5] or for surveillance and research in pre-clinical animal models. In intensive care research, it is often necessary to consider the entire organism and its metabolic connections. This emphasizes the utility of mouse models simulating clinical intensive care conditions, which can be performed at a reasonably large number of replicates, and allow postmortem exploration of involved and affected organs [6–10].

For studies involving larger animals, one may adapt breath sampling systems and equipment designed for human medicine. The key factors for analyzing the respiratory gas exchange rates (i.e., VO_2 and VCO_2) are calculated from the product of actual flow rates and concentration values for exactly the same points of time, which in turn requires precise alignment of the time profile of the concentration values and the gas flow. In humans, flow sensors and concentration sensors can be placed in parallel arrangement within the main gas stream [11], which still causes only minimal flow resistance due to the rather large diameter of the gas tubes of the respiratory system despite splitting the gas stream. However, a significant flow resistance will arise, if this main stream arrangement is scaled down for a gas line with a diameter of 1-3 mm, which requires positioning of the sensors one after another, and extensive corrections for the time offset during the measurements is required. During mechanical ventilation, mice require respiratory rates of approx. 150 cycles per minute, and a minute ventilation of 20 ml/min. Retracing a single breath cycle with 20 sampling points would therefore require a time resolution of 1 measurement every 20 msec. During that short time period, the mean gas release is approx. 7 µl. Such minuscule breath volumes do not meet the rather large sample volumes demanded by conventional analyzer systems designed for clinical applications. While capnography monitors adapted for use with rodents could handle the small volumes, they fail to provide O_2 measurements. Balances for O_2 uptake and CO_2 release for mice are typically assessed via so-called metabolic chambers [12]. However, due to the dead volume, the data obtained by these methods only provides coarse time averages of the net uptake and release [13]. Moreover, for obvious reasons the use of a metabolic chamber is not possible during mechanical ventilation.

At the current state-of-the-art, the authors are not aware of any approach that allows on-line breath gas monitoring with the small breath volumes available during mouse studies, which moreover are taking advantage of reasonably priced and ready-to-implement optical sensing strategies. As a compromise between breath-cycle resolved monitoring, and coarse time averages the present study focuses on a time scale resolution of one minute, which provides insight into the metabolic or physiologic response to a variety of deliberate experimental challenges. Consequently, we present a novel optical sensing system for routine online monitoring of exhaled breath in the mouse intensive care unit (MICU). This analyzer is based on a FTIR spectrometer equipped with a substrate integrated hollow waveguide (iHWG) pioneered by the Mizaikoff team [14,15]simultaneous serving as a miniaturized gas cell and IR photon conduit, and a luminescence - based flow-through oxygen sensor integrated into the respiratory equipment of the MICU. This sensing system offers an overall data sampling rate of one data point per minute. Previously optimized and now automated calibration algorithms and multivariate corrections/data evaluation routines including statistical sampling of measurement error offer rapid, reliable, and comfortable access to real-time data in routine operation with accurate and realistic error bounds at the demanded levels. The quality of measurements obtained with the developed system, and its potential to capture dynamic changes in the gas exchange is explored using exemplary mouse data.

2. Material and Methods

2.1. Experimental setup

The developed breath analyzer system comprises a custom-modified IR spectrometer for determining CO_2 via substrate-integrated hollow waveguides (iHWGs), and flow-cell-based luminescence sensors for oxygen measurements.

The IR component is based on a Bruker ALPHA FTIR Spectrometer (Bruker Optik GmbH, Ettlingen, Germany) equipped with a custom-made iHWG gas cell developed by the Mizaikoff team [16,17]. A 75 mm straight-channel iHWG with a channel cross-section of 2 mm^2 was simultaneously used as miniaturized gas cell, and as IR photon waveguide [14]. Using iHWGs is beneficial due to the minute required gas volume, their high volumetric optical efficiency, the rapid sampling rate, the possibility of temperature control, and their

mechanical stability [14,17–26]. Radiation from the IR spectrometer is focused into the iHWG, and propagated onto the internal DTGS detector of the ALPHA via two gold-coated off-axis parabolic mirrors (OAPM; diam: 1") with an effective focal length of 2" (Janos Technology Inc, Keene/NH, USA). A flow-through oxygen sensor (FireStingO2, Pyro Science GmbH, Aachen, Germany) is integrated into the gas outlet of the iHWG. Between measurements and during background collection, the iHWG is purged with synthetic air. A FlexiVent Module 1 respiratory system (Scireq, Montreal, Canada) is used for mechanical ventilation. A gas reservoir of approximately 100 mL is inserted between the expiratory branch of the respiratory system and the optical sensors, which serves as a damping element to smooth fluctuations in the gas concentration during a respiratory cycle. The developed breath analysis system was integrated into the existing respiratory system of the MICU unit, as shown in Fig.1.

2.2. Calibration design

The experimental design for calibrating the IR sensor consisted of a randomized set of 25 gas mixtures across the biologically expected concentration range of 1 - 5% CO2, and 20 - 80% oxygen, as can occur in ventilated patients. The combination and executed order of the samples was established using a full factorial design-of-experiment (DOE) (PLS Toolbox 7.9.3, Experiment Designer, Eigenvector Research, Inc., Manson/WA, USA). One mixture (1% CO2 / 20% oxygen) was repeated 5 times interspersed in the set to monitor changes of the system and of the mixing pump. This set was measured over 14 days, thereby resulting in 2700 data sets. The IR spectra were collected from 4000 – 400 cm^{-1} (averaging 20 background scans (nitrogen) and 20 sample scans; apodization function: Blackmann-Harris 3-Term, 5 or 10 repeats per mixture). The oxygen sensors were calibrated using 11 mixtures of oxygen and nitrogen spanning 0 – 100% oxygen, repeated over 19 days, resulting in 385 calibration data sets. The calibration is performed in dry gas (0% r.H./relative humidity), and at a flow of 200 mL/min. While flow effects are negligible, the oxygen sensor signal depends on the sample humidity. Expired air has a temperature of approx. 34°C and r.H. of 95%. With the transfer through the tubing, the air cools down to ambient temperature, and the humidity reaches saturation at 100% with some even condensing at the inner tube wall.

Fig. 3 shows the change in δφ signal of the oxygen sensor resulting from the relative humidity at concentration levels of 16% O_2. The humidity effect - when expressed as a change in the δφ signal - increases from zero to about 0.59 at saturation. The data for this correction was gained by an experiment where a mixture of 16 % O_2 was enriched in humidity by a humidity generator (Owlstone Humidity Generator OHG-4, Owlstone Inc., Cambride, UK) from close to 0 to 100 % r.H. and the signal measured by the same oxygen sensor as the one integrated into the setup. The humidity was measured using a capacitive humidity sensor (SF52, Mitchell Instruments, Ely, UK), where the dielectric strength of hygroscopic polymer is altered by the water vapor content.

The calibration of the sensor was performed using dry gas mixtures, since the accuracy of reference gases with a set humidity is questionable using gas bottles. It was assumed that the expired air should be saturated, and ideally the difference in humidity between breath gas and calibration sample should be 100%. With the transfer through the tubing, some humidity may be picked up by the calibration samples, and in turn some humidity may be lost for the respiration samples. Both processes reduce the difference between calibration and breath gas. While routine measurements of the relative humidity for each sampling point are not available, a difference of 95% between calibration gas and breath samples was assumed accounting for minor changes. According to Figure 3, this translates to a change in δφ of 0.59 ± 0.039. For data evaluation, each measurement of δφ was corrected for this offset, and an uncertainty of ± 0.039 was added next to the measurement error to each measurement, if the error propagation from raw measurements to O2 production and RQ values was estimated as outlined in Fig. 2.

Data evaluation was performed using MATLAB 8.6 (R2015b, The Mathworks Inc, Naticks/MA, USA), PLS Toolbox 7.9.3(Eigenvector Research, Inc., Manson/WA, USA) and MatlabStan 2.7.0.0 [27]/ Stan 2.11.0 [28].

All gas calibration samples were prepared from pure technical grade nitrogen, pure technical grade carbon dioxide and pure medical grade oxygen (all MTI Industriegase, Neu-Ulm, Germany) using a gas mixing pump (DIGAMIX 2M 301, H. Wösthoff Messtechnik GmbH, Bochum, Germany). For routine calibrations, three certified test gases were used: 5% CO_2 and 20% oxygen in nitrogen (Cal 1), 0.99% CO_2 and 29.9% oxygen in nitrogen(Cal2) and 2.49% CO_2 in nitrogen (Cal 3) (all MTI Industriegase, Neu-Ulm, Germany).

During mouse experiments, one CO_2 IR spectrum every minute, and one O_2 data point every second was obtained. The 60 oxygen data points were averaged for noise reduction, thus resulting in one final time-synchronized data point for oxygen and carbon dioxide every minute during online mouse breath monitoring. Prior to starting routine measurements, an IR background was sampled using ambient air. After around half-time of an average mouse experiment (i.e., after approximately 3 h), the sensor measurements were stopped for a short period enabling to record a new IR background. For daily calibration, five IR spectra and at least 100 oxygen data points of the two/three calibration gases were recorded at the end of the procedure and averaged. The system reaches a dynamic range for calibration (i.e., ignoring humidity) of 1 to 5 % for carbon dioxide, and 10 to 90 % for oxygen. The system was humidity calibrated for 16 % oxygen, which is the usual oxygen content in exhaled breath of mice using air as the inspiratory gas mixture.

2.3. Data analysis procedure

The data analysis routine was based on a calibration transfer algorithm previously developed and optimized by the authors for the present optical sensing system [29,30]. This data analysis strategy is based on hierarchical Bayesian models and Lagrange Multiplier optimization. Monte-Carlo Markov Chain sampling provides realistic estimates for coefficients and prediction together with accurate error bounds by simulating known measurement errors and system fluctuations. Using only three calibration gases, both the FTIR system and the oxygen sensors are simultaneously calibrated for daily routine use. Fully automated Matlab scripts and wrappers offer comfortable and rapid data evaluation for routine studies without the requirement of expert users.

Fig. 2 provides an outline of the data evaluation model including its error propagation scheme. The day-to-day variance (i.e., represented by the calibration sets used to build the hierarchical model), the knowledge gained on the fit equation, and the fit coefficients gained by the hierarchical model, and actual calibration samples analyzed to represent the current sensor status were used to build the actual calibration model by using a calibration transfer algorithm based on Lagrange Multiplier optimization. Combined with the sensor signal, concentrations of the breath markers are calculated. The corresponding uncertainty estimation derives from the uncertainty in calibration coefficients as well as from modeling of the current random measurement error from the actual calibration samples and sensor

response. Readers interested in the full error propagation procedure are referred to the supplementary material.

The calibration of the oxygen sensor is based on an empirical rational function following

$$\delta\varphi = \frac{c_1[O_2]^2 + c_2[O_2] + c_3}{[O_2] + c_4} \quad (2)$$

with δφ representing the raw data recorded by the oxygen sensor. This value is corrected for an offset in δφ expected for a difference of 95% r.H between the calibration samples and the breath samples. $[O_2]$ refers to the oxygen concentration in vol%, and c_i to the current calibration coefficients. The uncertainty in the humidity values is considered as a propagation of errors from the measurements and other sources, as depicted in Figure 2. Here, random δφ offset values in the range of 0.59 ± 0.039 were generated, whereby the ± 0.039 variability covers both an uncertainty in humidity difference and in calibration slope.

The IR data evaluation uses the main IR absorption peak of CO_2, and is first applying a data reduction routine via principal component analysis (PCA) to one score, and then correcting for other interferents (i.e., oxygen) via the corresponding response surface. The calibration equation therefore writes as follows:

$$S = c_1 + c_2[CO_2] + c_3[CO_2]^2 + c_4[O_2][CO_2] \quad (3)$$

with S score of principal component 1, $[CO_2]$ the carbon dioxide concentration in vol%, $[O_2]$ the oxygen concentration in vol%, and c_i the current calibration coefficients. More detailed information can be found in our associated previous studies [29,30]. Next to the exhaled oxygen and carbon dioxide concentration directly obtained from the two sensor systems, the difference between inhaled and exhaled oxygen, i.e., ΔO_2 describes the amount of consumed oxygen, and is another relevant metabolic parameter. Since in the current MICU setup, the mouse is ventilated using compressed air, the inhaled oxygen concentration is determined by analyzing the oxygen content in compressed air. The entire calibration procedure is visually summarized in Fig. 4. By using the large number of sampling iterations gained from Stan software, it is possible to calculate the average, standard deviation and 95 % confidence interval values, thereby offering robust and realistic error boundaries for all calculated values.

3. Animal experiments

The study was approved by the federal authorities for animal research of the Regierungspräsidium Tübingen (approved animal experimentation number: 1190, 24.09.2014), Baden-Württemberg, Germany, and the Animal Care Committee of the University of Ulm, Baden-Württemberg, Germany, and performed in adherence with the National Institutes of Health Guidelines on the Use of Laboratory Animals and the European Union ‘‘Directive 2010/63 EU on the protection of animals used for scientific purposes.

The study was conducted during the year 2016, and was recently published [31], where anesthesia, surgical instrumentation and the experimental design have been discussed in detail. Animals were mechanically ventilated with a small animal ventilator (FlexiVent, Scireq, MO, Canada) using a pressure-controlled mode. Initial ventilator settings were F_iO_2 0.21, respiratory rate 150·min^{-1}, tidal volume 4 to 6mL g^{-1}, inspiratory/expiratory time ratio 1:2, and positive end-expiratory pressure (PEEP) 3cmH_2O. The respiratory rate was modified to maintain an arterial partial pressure of CO_2 ($paCO_2$) between 30 and 40 mmHg, and the PEEP was varied according to the arterial paO_2 (if paO_2/F_iO_2>300mmHg: PEEP=3cmH_2O; paO_2/F_iO_2<300mmHg: PEEP=5cmH_2O; paO_2/F_iO_2<200 mmHg: PEEP=8cmH_2O). Recruitment maneuvers (RM, 5s hold at 18cmH_2O) were repeated every 30 min to avoid atelectasis formation due to the anesthesia and supine positioning. Each hour, the RM was followed by a compliance measurement, where the lung was inflated to a volume of 1 ml and the thoracial pressure was measured. Thereafter, a second RM was performed. General anesthesia was sustained by continuous intravenous administration of ketamine, midazolam, and fentanyl to reach deep sedation. The experiment started with a thorax trauma, followed by surgical instrumentation. Hemorrhagic shock was performed about one hour later by removing 30µL·g-1 of blood and by titrating mean arterial pressure (MAP) to 35mmHg via further removal or retransfusion of blood. Fluid administration was temporarily stopped. At the start of the resuscitation phase, shed blood was re-transfused, together with the administration of hydroxyethyl starch 6% and noradrenaline (NA) titrated to maintain MAP≥50mmHg. At the end of the experiment, animals were exsanguinated via blood withdraw from the arterial catheter under deep anesthesia.

4. Results and discussion

The data presented are that of one animal (wild type C57BL/6J strain) of the study group, undergoing a combined blunt chest trauma and hemorrhagic shock.

4.1. Physiology and metabolism

The data analysis provides inhaled and exhaled oxygen concentration, their difference (ΔO_2), and the exhaled carbon dioxide concentration which together allow estimating the respiratory quotient in exhaled mouse breath. The experiment started around 8:00 and ended approximately seven hours later delivering one data point per minute on the current metabolic status of the mouse. Fig. 5 shows the determined respiratory concentration data. After thorax trauma, arterial and central venous catheters were implemented for monitoring and drug administration. Then the mouse was connected to the ventilation system, while breath gas recording was initiated a bit before, in order not to hinder medical procedures. This connection is reflected in a first jump of the measured O_2 consumption, as shown in Figure 5c. Continuous recording was maintained until the mouse died, which coincided with a sharp drop of O_2 consumption. The first connection was followed by a ragged time course for both O_2 consumption and CO_2 production. The ragged time course was due to 'recruitment maneuvers' [32,33] (denoted in the following as RM) which started 100 minutes after beginning and were repeated in an interval of 30 min. RMs were used in mice during mechanical ventilation with low tidal volumes, in order to re-expand at electatic lung regions, which had collapsed due supine positioning, anesthesia effects and reduced diaphragmatic muscle tone, and thereby restore and/or maintain static thoraco-pulmonary compliance [34]. RMs are characterized by a transient increase of the airway pressure during a couple of seconds, which will re-open non or poorly aerated alveoli. As a consequence, respiratory system mechanics and gas exchange are improved. Beside the intermittent peaks, the time course of the RQ data shows a significant drop to values close to 0.7 towards the end of the protocol. The down-drift of the RQ values lasts for 3-4 hours. For such a long period, the CO_2 output by respiration has to match the CO_2 production by oxidation. Any increase in tissue/blood CO_2 content may subsequently induce hemodynamic variations, because CO_2 is well established as potent systemic vasodilator as well as a pulmonary vasoconstrictor. The down drift indicates an increasing preference for fat oxidation with increasing duration of the experiment, and thus rules out respiratory effects

of hypoventilation, which act on a shorter time scale. However, acute variations in the gas exchange are evident in response to the intermittent RMs. Fig. 6 takes a closer look at the O_2 uptake data during a RM. It demonstrates a sharp drop in the O_2 uptake in response to a RM that lasts about 5 minutes, followed by a steady increase towards the level that was observed just before the maneuver. The reduced uptake in the first phase of the maneuver may result from two phenomena, First, an enforced 'breath holding' that last for a few seconds. The observed response may last longer as it is stretched out with the damping reservoir that is inserted in the expiratory branch of the measurement system. The second process is linked to high intrathoracic pressures that were induced with RMs, which may have a detrimental effect on cardiac output [35], and may thereby reduce pulmonary perfusion and impair the gas exchange. The rebound in pulmonary perfusion may explain the recovery of the O_2 uptake that is seen about 10 minutes after a RM. Figure 6b indicates that this pattern is reproducible for repetitive RMs. The expiratory CO_2 release follows the same pattern except that transient increase evident in the first response to a RM. It can be explained by a CO_2 accumulation during the 'breath holding' phase, and a transiently increased washout of CO_2 directly after a RM most likely due to the RM-induced transitory increase in alveolar ventilation.

After the first RM, approx. 2 hours after beginning a hemorrhagic shock was induced which lasted for one hour. The reduced blood volume during shock causes a reduced organ perfusion and thereby reduced oxygen supply. An oxygen supply/demand mismatch may develop, which is considered to be key determinant of hemorrhagic damage [36,37], and should be reflected in a transient drop of the O_2 uptake. Fig. 6 shows a smoothed uptake curve that was tentatively corrected for the perturbations caused by RMs. The first response to the hemorrhagic shock is superimposed by effects of a RM performed five minutes earlier, which complicates such a correction. Nevertheless, the corrected uptake curve shows a drop to minimal O_2 uptake values during hemorrhagia and a subsequent compensatory increase. The data shown so far give a hint about the information that can be obtained with continuous monitoring of respiratory O_2 and CO_2 data.

4.2. Precision and accuracy in RQ determinations

Figure 5 demonstrates how RQ values are derived from O_2 and CO_2 concentration measurements, and the effect of humidity on these estimates. According to figure 3, an

increase in humidity from zero to 100% increases the δφ signal by 0.6, which translates to an approximate decrease of 16 % to 15.3% in the O_2 concentration. In consequence, the breath gas measurements are underestimated, and correcting this shift increases the average O_2 in mouse breath concentration measurement by approximately 0.7%. This is reflected in Fig. 5, which shows the results with and without correction side-by-side. As expected, there is no significant influence on the CO_2 quantification, however, the exhaled oxygen values are raised by the oxygen correction. Subsequently, ΔO_2 is lowered, and RQ is raised. This is actually a desired result, since in other mice data the RQ was sometimes below the biological limit of 0.6, which indicates that it was underestimated. Actual r.H. values cannot be determined during routine experiments. Therefore, it was assumed that the difference in r.H. for breath gas measurements and calibration gas measurements fluctuates in the range of 95 ± 3%. These fluctuations should translate into variations of ± 0.039 in the δφ signal, and ± 0.059 in the O_2 concentrations; correspondingly, the RQ estimates fluctuate likewise.

The uncertainty in the breath sample humidity is captured in a sequence of (Bayesian MCMC) sampling runs, which were generated to assess the error propagation. For each sample run, simulated random fluctuations of humidity were used for correction and combined with simulated measurement errors and the resulting 'noisy' data were used to assess the RQ values.

There are two sources of fluctuations that affect the estimated RQ values. One source relates to per-second or per-minute fluctuations in the sensor signals for O_2 and CO_2, and are called 'short-term fluctuations'. The other source are uncertainties in the coefficients for the calibration curves of O_2 and CO_2. These values fluctuate from day-to-day, yet were constant during any given measurement day. These uncertainties are referred to as 'long-term fluctuations'.

Based on the sampling strategy, r.H. is assigned to the long-term fluctuations. If one is primarily interested in changes of the RQ values with time or in response to an experimental intervention such as the hemorrhagic shock, then long-term fluctuations may safely be ignored, and the fixed values for the mean calibration coefficients and humidity corrections can be used. To isolate the effect of long-term vs. short-term fluctuations, simulations were performed where different fluctuations were turned off. Figure 7 shows the resulting confidence ranges for a time section of the protocol. If only short-term fluctuations are considered, then the uncertainty in RQ determinations

is reduced by 50%. Ignoring the effect of the relative humidity reduces the uncertainty to approx. 2/3 of the initial starting values. If short-term fluctuations were ignored but all long-term variations considered, barely any improvement is evident. This can be explained by the fact that the variances of the fluctuation add up, however, not their standard deviation. In other words, the overlay of one source with a fluctuation (i.e., a standard deviation; SD) of 0.2 with a variable that has a SD of 1.0 results in an overlaid standard deviation of 1.02. These data indicate that the precision (i.e., approx. twice the SD) in absolute values for RQ estimates is approx. ± 0.04 or less than 5% of the nominal value. Schadewaldt et al. [37] explored the precision in RQ estimates of commercial instruments including the former 'Deltatrac' gold-standard. They found precision values, which were about twice the values determined in the present study with the system developed herein. Our data indicate that imprecision in long-term factors evidently play a major role. If one is primarily interested in changes in respiratory values observed in response to a challenge, fluctuations may be ignored, which almost doubled the precision. Our study furthermore demonstrates that these responses cover metabolic changes caused by a hemorrhagic shock, and serve as indicators of an inflicted damage [35,36]. The extent of a drop in O_2-uptake following a recruitment maneuver reflects the vulnerability of the circulatory system and cardiac function [34]. Hence, the approach developed in the course of this study is a viable strategy to assess the O_2/CO_2 gas exchange, and its dynamic alterations. Thus, a valuable tool for characterizing the underlying metabolic and physiologic conditions has been established and will be further evolved for widespread routine usage.

5. Conclusions and outlook

In this study, an innovative optical sensor system is presented combining infrared and luminescent sensing principles for on-line monitoring relevant metabolic parameters (i.e., exhaled oxygen and carbon dioxide, difference between inhaled and exhaled oxygen and the respiratory quotient) in the exhaled breath of ventilated mice at a temporal resolution of one data point per minute. Thereby, the immediate metabolic status of the mouse during medical trials may be continuously monitored. It was shown that continuous monitoring may reliably capture actual values of the respiratory quotient with a 95% confidence interval of ± 0.04. Moreover, an unexpected sensitivity of RQ values against recruitment maneuvers was

revealed for the first time via the developed sensing strategy, which may be indicative for pulmonary or circulatory problems and will be investigated in more detail during future studies.

The developed optical sensing system comprises a modified FTIR spectrometer combined with a substrate-integrated hollow waveguide (iHWG) and a luminescence - based flow-through oxygen sensor integrated into the respiratory system of a mouse intensive care unit (MICU). Optimized and automated calibration routines along with statistical sampling offer a rapid, reliable and comfortable data evaluation strategy providing accurate and realistic error boundaries resulting from average, standard deviation and 95 % confidence interval values at each data point.

The developed system is nowadays in daily use at the MICU located at Institute of Anesthesiologic Pathophysiology and Method Development at Ulm University Medical Center continuously proving the reliability of the developed system in routine exhaled breath analysis scenarios.

6. Acknowledgements

The authors deeply acknowledge continuous support of the team operating the mouse intensive care unit (MICU) at the Institute of Anesthesiologic Pathophysiology and Method Development at the Ulm University Medical Center for assistance during the mouse breath studies. The authors would like to furthermore thank the Federal State of Baden-Württemberg (Landesgraduiertenförderungsgesetz, grant number: 1212-LGFG-E) for partial financial support to FS. The development of the sensing technology was performed in part under the auspices of the U.S. Department of Energy by Lawrence Livermore National Laboratory (LLNL) under Contract DE-AC52-07NA27344. This project was partially funded under LLNL sub-contract Nos. B598643 and B60301. The Boehringer Ingelheim Ulm University BioCenter (BIU, grant number: D.5008) is acknowledged for financial support. The animal studies were in part supported by a SFB-Grant of the Germany research foundation (DFG, Grant number 1149). Last but not least, the BMBF project APOSEMA and MSCA RISE project TROPSENSE (funded by the Horizon 2020 Framework Programme of the European Union under grant agreement n° 645758) are acknowledged for partial financial support.

The authors declare no conflict of interest and that the funding agencies had no influence on the work presented and on the publication of this paper.

[1] A. Amann, D. Smith, Breath Analysis for Clinical Diagnosis and Therapeutic Monitoring, World Scientific, 2005.

[2] S. Bursztein, P. Saphar, P. Glaser, U. Taitelman, S. de Myttenaere, R. Nedey, Determination of energy metabolism from respiratory functions alone., J. Appl. Physiol. 42 (1977) 117–119. doi:10.1152/jappl.1977.42.1.117.

[3] P.C. Even, N.A. Nadkarni, Indirect calorimetry in laboratory mice and rats: principles, practical considerations, interpretation and perspectives., Am. J. Physiol. Regul. Integr. Comp. Physiol. 303 (2012) R459-76. doi:10.1152/ajpregu.00137.2012.

[4] E.E.M. da Rocha, V.G.F. Alves, R.B. V da Fonseca, Indirect calorimetry: methodology, instruments and clinical application., Curr. Opin. Clin. Nutr. Metab. Care. 9 (2006) 247–256. doi:10.1097/01.mco.0000222107.15548.f5.

[5] C.A. Wyse, K.D. Slceldon, A.J. Cathcart, R. Sutherland, S.A. Ward, G. Gibson, L.C. McMillan, M.J. Padgett, T. Preston, P.S. Yam, S. Love, Breath Analysis: Taking the Needle Out of Veterinary Diagnostics?, in: A. Amann, D.S. Keele (Eds.), World Scientific, New Jersey, 2005.

[6] G. Albuszies, P. Radermacher, J. Vogt, U. Wachter, S. Weber, M. Schoaff, M. Georgieff, E. Barth, Effect of increased cardiac output on hepatic and intestinal microcirculatory blood flow, oxygenation, and metabolism in hyperdynamic murine septic shock, Crit. Care Med. 33 (2005) 2332–2338.

[7] V. Simkova, K. Baumgart, J.A. Vogt, U. Wachter, S. Weber, M. Gröger, G. Speit, P. Radermacher, G. Albuszies, E. Barth, The effect of superoxide dismutase overexpression on hepatic gluconeogenesis and whole-body glucose oxidation during resuscitated normotensive murine septic shock., Shock. 30 (2008) 578–84. doi:10.1097/SHK.0b013e31816a6e0f.

[8] K. Baumgart, V. Simkova, F. Wagner, S. Weber, M. Georgieff, P. Radermacher, G. Albuszies, E. Barth, Effect of SOD-1 over-expression on myocardial function during

resuscitated murine septic shock, Intensive Care Med. 35 (2009) 344–349.

[9] K. Baumgart, F. Wagner, M. Gröger, S. Weber, E. Barth, J. Vogt, U. Wachter, M. Huber-Lang, M.W. Knöferl, G. Albuszies, M. Georgieff, P. Asfar, C. Szabo, E. Calzia, P. Radermacher, V. Simkova, Cardiac and metabolic effects of hypothermia and inhaled hydrogen sulfide in anesthetized and ventilated mice, Crit. Care Med. 38 (2010) 588–595. doi:10.1097/CCM.0b013e3181b9ed2e.

[10] K. Wagner, M. Groger, O. McCook, A. Scheuerle, P. Asfar, B. Stahl, M. Huber-Lang, A. Ignatius, B. Jung, M. Duechs, P. Moller, M. Georgieff, E. Calzia, P. Radermacher, F. Wagner, Blunt Chest Trauma in Mice after Cigarette Smoke-Exposure: Effects of Mechanical Ventilation with 100% O2, PLoS One. 10 (2015) e0132810.

[11] L. Ciaffoni, G. Hancock, J.J. Harrison, J.P.H. Van Helden, C.E. Langley, R. Peverall, G.A.D. Ritchie, S. Wood, Demonstration of a mid-infrared cavity enhanced absorption spectrometer for breath acetone detection, Anal. Chem. 85 (2013) 846–850. doi:10.1021/ac3031465.

[12] J. Joo, C. Cox, E. Kindred, L. Lashinger, M. Young, M. Bray, The acute effects of time-of-day-dependent high fat feeding on whole body metabolic flexibility in mice, Int. J. Obes. 40 (2016) 1444–1451.

[13] J. Lighton, Limitations and requirements for measuring metabolic rates: a mini review, Eur. J. Clin. Nutr. 71 (2017) 301–305.

[14] A. Wilk, J. Chance Carter, M. Chrisp, A.M. Manuel, P. Mirkarimi, J.B. Alameda, B. Mizaikoff, Substrate-integrated hollow waveguides: A new level of integration in mid-infrared gas sensing, Anal. Chem. 85 (2013) 11205–11210. doi:10.1021/ac402391m.

[15] J.C. Carter, M.P. Chrisp, A.M. Manuel, B. Mizaikoff, A. Wilk, S.-S. Kim, Substrate-integrated hollow waveguide sensors., US20130081, 2013.

[16] P.R. Fortes, J.F. da Silveira Petruci, A. Wilk, A.A. Cardoso, I.M. Raimundo Jr, B. Mizaikoff, J. Flávio, I. Milton, R. Jr, Optimized design of substrate-integrated hollow

waveguides for mid-infrared gas analyzers, J. Opt. 16 (2014) 94006. doi:10.1088/2040-8978/16/9/094006.

[17] P.R. Fortes, J.F. da Silveira Petruci, A. Wilk, A.A. Cardoso, I.M. Raimundo Jr, B. Mizaikoff, Optimized design of substrate-integrated hollow waveguides for mid-infrared gas analyzers, J. Opt. 16 (2014) 94006. doi:10.1088/2040-8978/16/9/094006.

[18] I. José Gomes da Silva, E. Tütüncü, M. Nägele, P. Fuchs, M. Fischer, I.M. Raimundo, B. Mizaikoff, Sensing hydrocarbons with interband cascade lasers and substrate-integrated hollow waveguides, Analyst. 141 (2016) 4432–4437. doi:10.1039/C6AN00679E.

[19] M. Sieger, B. Mizaikoff, Optimizing the design of GaAs/AlGaAs thin-film waveguides for integrated mid-infrared sensors, Photonics Res. 4 (2016) 106. doi:10.1364/PRJ.4.000106.

[20] R.L. Ribessi, T. de A. Neves, J.J.R. Rohwedder, C. Pasquini, I.M. Raimundo, A. Wilk, V. Kokoric, B. Mizaikoff, iHEART: a miniaturized near-infrared in-line gas sensor using heart-shaped substrate-integrated hollow waveguides, Analyst. 141 (2016) 5298–5303. doi:10.1039/C6AN01027J.

[21] E. Tütüncü, M. Nägele, P. Fuchs, M. Fischer, B. Mizaikoff, iHWG-ICL: Methane Sensing with Substrate-Integrated Hollow Waveguides Directly Coupled to Interband Cascade Lasers, ACS Sensors. (2016) acssensors.6b00238. doi:10.1021/acssensors.6b00238.

[22] E. Tütüncü, V. Kokoric, R. Szedlak, D. MacFarland, T. Zederbauer, H. Detz, A.M. Andrews, W. Schrenk, G. Strasser, B. Mizaikoff, Advanced gas sensors based on substrate-integrated hollow waveguides and dual-color ring quantum cascade lasers, Analyst. 141 (2016) 6202–6207. doi:10.1039/C6AN01130F.

[23] V. Kokoric, A. Wilk, B. Mizaikoff, iPRECON: an integrated preconcentrator for the enrichment of volatile organics in exhaled breath, Anal. Methods. 7 (2015) 3664–3667. doi:10.1039/C5AY00399G.

[24] J.F. da S. Petruci, A. Wilk, A.A. Cardoso, B. Mizaikoff, Online Analysis of H2S and

SO2 via Advanced Mid-Infrared Gas Sensors., Anal. Chem. (Washington, DC, United States). 87 (2015) 9605–9611.

[25] J.F.D.S. Petruci, P.R. Fortes, V. Kokoric, A. Wilk, I.M. Raimundo, A.A. Cardoso, B. Mizaikoff, Monitoring of hydrogen sulfide via substrate-integrated hollow waveguide mid-infrared sensors in real-time., Analyst. 139 (2014) 198–203. doi:10.1039/c3an01793a.

[26] D. Perez-Guaita, V. Kokoric, A. Wilk, S. Garrigues, B. Mizaikoff, Towards the determination of isoprene in human breath using substrate-integrated hollow waveguide mid-infrared sensors, J. Breath Res. 8 (2014) 26003. doi:10.1088/1752-7155/8/2/026003.

[27] B. Lau, MatlabStan: the MATLAB interface to Stan, (2015). http://mc-stan.org/matlab-stan.html.

[28] B. Carpenter, A. Gelman, M. Hoffman, D. Lee, B. Goodrich, M. Betancourt, M.A. Brubaker, P. Li, A. Riddell, Journal of Statistical Software Stan : A Probabilistic Programming Language, J. Stat. Softw. VV (2016).

[29] F. Seichter, J. Vogt, P. Radermacher, B. Mizaikoff, Nonlinear calibration transfer based on hierarchical Bayesian models and Lagrange Multipliers: Error bounds of estimates via Monte Carlo – Markov Chain sampling, Anal. Chim. Acta. 951 (2016) 32–45. doi:10.1016/j.aca.2016.11.025.

[30] F. Seichter, J. Vogt, P. Radermacher, B. Mizaikoff, Response-surface fits and calibration transfer for the correction of the oxygen effect in the quantification of carbon dioxide via FTIR spectroscopy, Anal. Chim. Acta. 972 (2017). doi:10.1016/j.aca.2017.03.053.

[31] C. Hartmann, M. Groger, J.-P. Noirhomme, A. Scheuerle, P. Moller, U. Wachter, M. Huber-Lang, B. Nussbaum, B. Jung, T. Merz, O. McCook, S. Kress, B. Stahl, E. Calzia, M. Georgieff, P. Radermacher, M. Wepler, In-Depth Characterization of the Effects of Cigarette Smoke Exposure on the Acute Trauma Response and Hemorrhage in Mice., Shock. (2018). doi:10.1097/SHK.0000000000001115.

[32] C.M. Lim, H. Jung, Y. Koh, J.S. Lee, T.S. Shim, S.D. Lee, W.S. Kim, D.S. Kim, W.D. Kim, Effect of alveolar recruitment maneuver in early acute respiratory distress syndrome according to antiderecruitment strategy, etiological category of diffuse lung injury, and body position of the patient, Crit. Care Med. 31 (2003) 411–418.

[33] L.K. Reiss, A. Kowallik, S. Uhlig, Recurrent recruitment manoeuvres improve lung mechanics and minimize lung injury during mechanical ventilation of healthy mice, PLoS One. 6 (2011). doi:10.1371/journal.pone.0024527.

[34] M. Biais, R. Lanchon, M. Sesay, L. Le Gall, B. Pereira, E. Futier, K. Nouette-Gaulain, Changes in Stroke Volume Induced by Lung Recruitment Maneuver Predict Fluid Responsiveness in Mechanically Ventilated Patients in the Operating Room, Anesthesiology. 126 (2017) 260–267.

[35] D. Rixen, J.H. Siegel, Bench-to-bedside review: oxygen debt and its metabolic correlates as quantifiers of the severity of hemorrhagic and post-traumatic shock, Crit. Care. 9 (2005) 441–453.

[36] R.W. Barbee, P.S. Reynolds, K.R. Ward, Assessing shock resuscitation strategies by oxygen debt repayment, Shock. 33 (2010) 113–122.

[37] P. Schadewaldt, B. Nowotny, K. Strassburger, J. Kotzka, M. Roden, Indirect calorimetry in humans: a postcalorimetric evaluation procedure for correction of metabolic monitor variability, Am. J. Clin. Nutr. 97 (2013) 763–773.

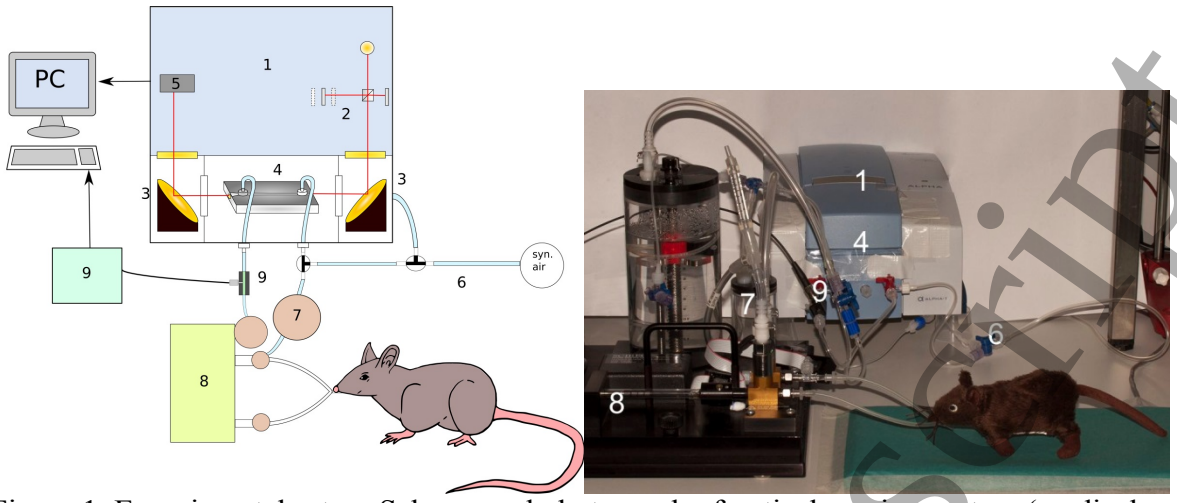

Figure 1. Experimental setup: Scheme and photograph of optical sensing system (medical instrumentation not completely shown). A compact FTIR spectrometer (1) was customized with an iHWG gas cell (4). IR radiation was in/outcoupled via adjustable gold-coated off-axis parabolic mirrors (OAPMs, 3). A fluorescence-based flow-through oxygen sensor (9) was connected to the output of iHWG. The optical sensing system was fully integrated into the ventilation module of the anesthetized and sedated, unconscious mouse (catheter and syringe pumps not shown) within the mouse intensive care unit (MICU).
Legend of system components: 1) FTIR Spectrometer, 2) Interferometer, 3) OAPM, 4) iHWG, 5) IR detector (deuterated triglycine sulfate, DTGS), 6) Air supply and spectrometer/iHWG purging, 7) 100 ml vial as dampening element of respiratory system, 8) respiratory system of the MICU, 9) oxygen sensor (catheters, needles syringe pumps for venipuncture, urine draw and sedation/anesthesia, and medication not shown).

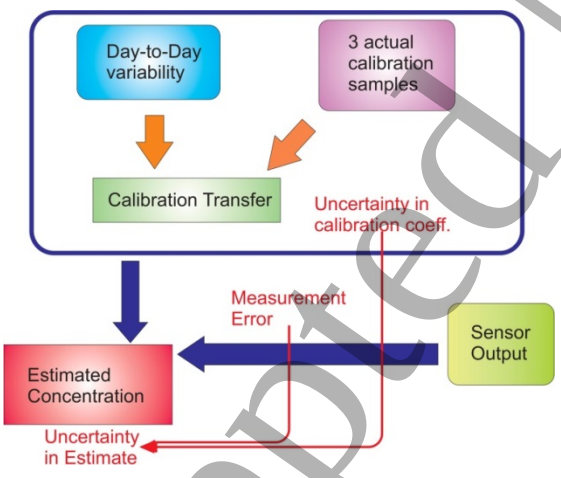

Figure 2. Schematic flow-chart of the calibration and data analysis routine. The routine was developed for providing a complete error propagation (both for oxygen and carbon dioxide calibration) caused by the uncertainty in the coefficients of a calibration function, which were derived from previous studies and the actual measurement error for the 3 calibration samples used herein. The error propagation was estimated based on a statistical Bayesian model using the Stan software package.

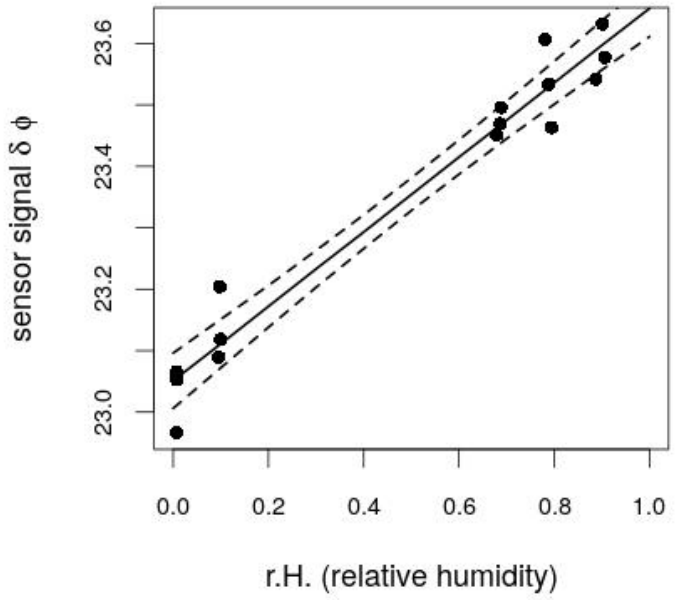

Figure 3: Calibration of the effect of humidity on the measured δφ signal of the oxygen sensor. The offset of δφ values was assessed as slope of the calibration curves times 0.95, the expected difference of humidity in calibration samples and actual breath samples. The dotted lines show the 95 % confidence interval.

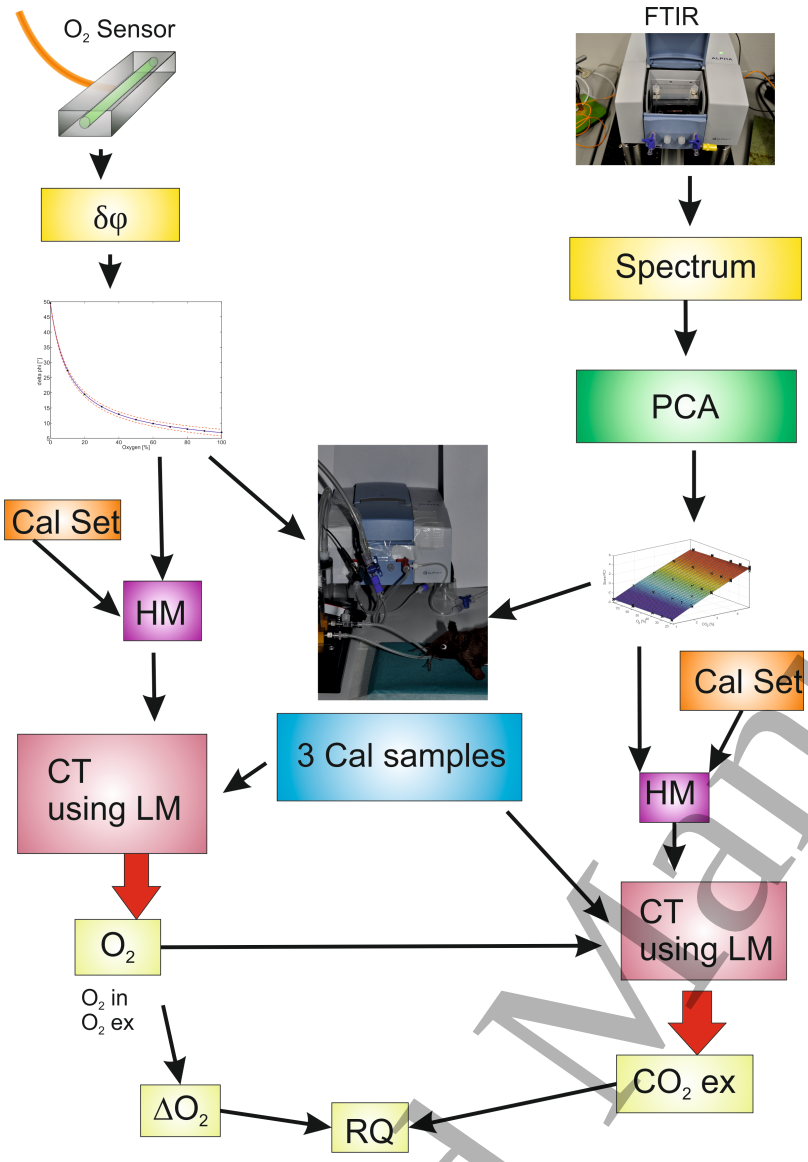

Figure 4: Visual flow chart of the calibration and data analysis procedure. Black arrows represent data passing onto a next processing step. The values in the light green boxes (O_2 in, O_2 ex, CO_2 ex, ΔO_2, RQ) are the parameters gained by the data analysis procedure during a measurement cycle. FTIR: Fourier-transform Infrared spectrometer, δφ: raw value of oxygen sensor, PCA: Principal Component Analysis, Cal Set: calibration sets used for building the model, HM: hierarchical model, CT: calibration transfer, LM: Lagrange multiplier optimization approach, Cal Samples: actual calibration samples analyzed (i.e., daily calibration), O_2 in: inhaled oxygen concentration, O_2 ex: exhaled oxygen concentration, CO_2 ex: exhaled carbon dioxide concentration, ΔO_2 :difference between inhaled and exhaled oxygen, RQ: respiratory quotient

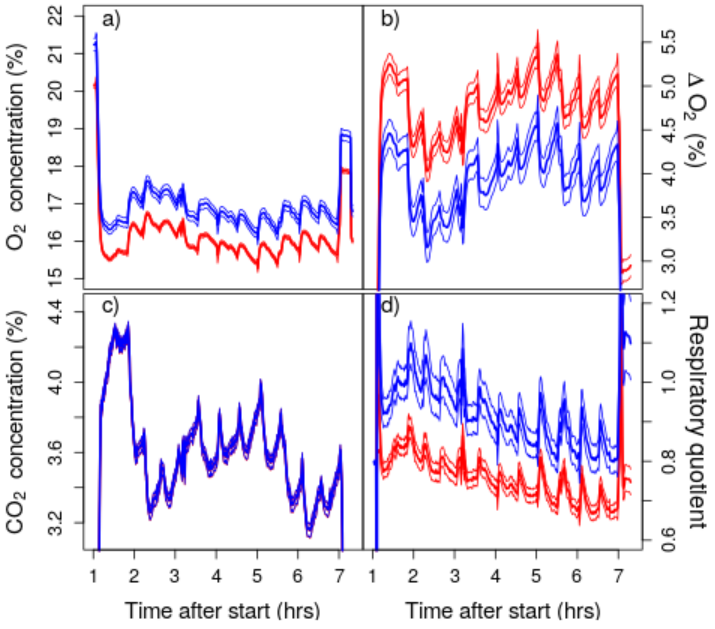

Figure 5. Exemplary results of one mouse experiment: a) Exhaled oxygen; b) Difference between inhaled and exhaled oxygen; c) Exhaled carbon dioxide; d) Respiratory quotient. Thicker solid line: mean, thinner solid line: 95 % confidence interval. Red: no correction, blue: with humidity correction.

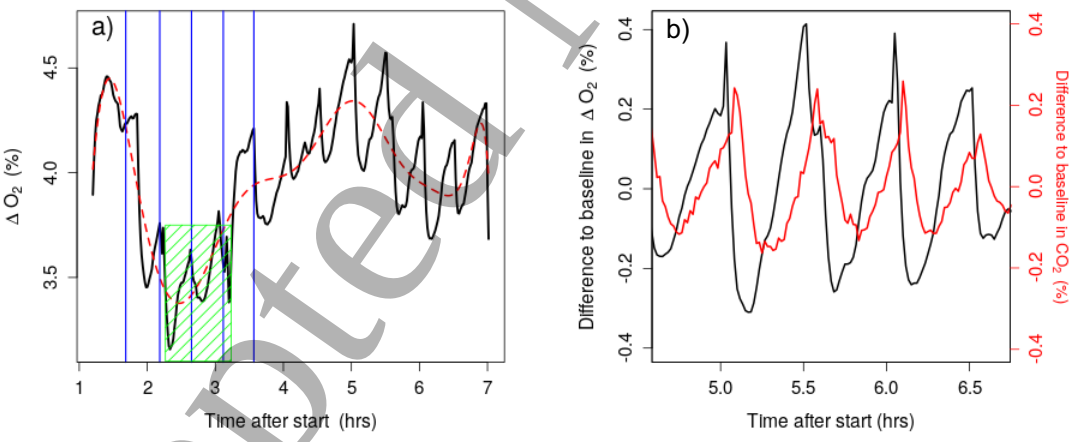

Figure 6: Physiologic interpretation of the results. a) Time course of the O_2 uptake and a tentative correction for the effect of intermittent recruitment maneuvers to expose the impact of a hemorrhagic shock. Black solid line: measured difference between the O_2 concentrations of inspired and expired air. Red dotted line: tentative interpolated function. The green area indicates the time frame of a hemorrhagic shock. b) CO_2 production and O_2 consumption during several recruitment maneuvers.

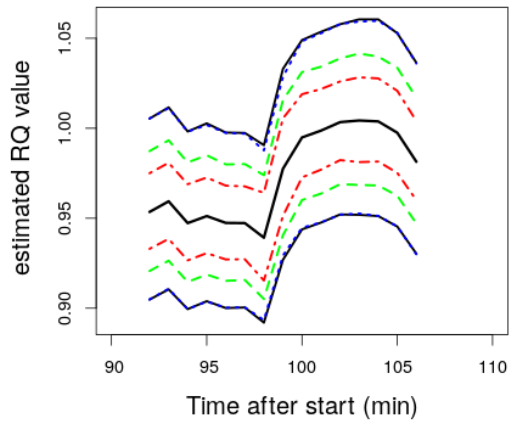

Figure 7: Impact of various random noise sources on the confidence range of the estimated RQ values. Black solid lines: mean values and confidence range considering all sources of fluctuations. Red dash-dotted line: only short-term effects, green dashed line: ignoring uncertainties in relative humidity. Blue dotted line: ignoring short-term fluctuations.